

Anodic Oxidation of Carbon Steel at High Current Densities and Investigation of Its Corrosion Behavior



ARASH FATTAH-ALHOSSEINI and HAMID YAZDANI KHAN

This work aims at studying the influence of high current densities on the anodization of carbon steel. Anodic protective coatings were prepared on carbon steel at current densities of 100, 125, and 150 A/dm² followed by a final heat treatment. Coatings microstructures and morphologies were analyzed using X-ray diffraction (XRD) and scanning electron microscope (SEM). The corrosion resistance of the uncoated carbon steel substrate and the anodic coatings were evaluated in 3.5 wt pct NaCl solution through electrochemical impedance spectroscopy (EIS) and potentiodynamic polarization measurements. The results showed that the anodic oxide coatings which were prepared at higher current densities had thicker coatings as a result of a higher anodic forming voltage. Therefore, the anodized coatings showed better anti-corrosion properties compared to those obtained at lower current densities and the base metal.

DOI: 10.1007/s11663-017-0943-7

© The Minerals, Metals & Materials Society and ASM International 2017

I. INTRODUCTION

THERE are several methods that have been developed to form protective oxides on steels such as thermal, chemical, and electrochemical oxidation.^[1] Anodic oxidation, so called anodizing, is a simple straightforward method for the production of oxide coatings on the surface of valve metals including Al, Ti, Zr, Hf, W, Nb, V, Zn, and Ta by electrolytic treatment in a suitable solution, which might inhibit the corrosion. Only for aluminum and its alloys and to a lesser extent magnesium, corrosion resistance can be dramatically enhanced by anodic formation of a dense oxide film on a commercial scale.^[2,3]

Several studies in the literature have reported the anodization of pure iron^[4–9] and carbon steels^[10,11] in alkaline solutions or ethylene glycol containing NH₄F and water for different purposes. Iron oxide films have important applications in electrochemical energy storage,^[12] electrohydrodynamic lithography (EHL),^[13] electrochemical supercapacitors,^[14] and coatings.^[15–18] The natural rust is generally a flaky, porous, friable substance, and it provides no protection to the underlying iron-like passive oxide films. Hematite (α -Fe₂O₃) is known as the main component of iron rust, which forms spontaneously when iron or an alloy that contains iron, is exposed to oxygen and air moisture for a long period of time.^[19,20] On the contrary, the magnetite coating which was formed by anodization process act as a dense barrier-type film and it can prevent or minimize the corrosion on iron or steel surface.^[21–24]

Burleigh *et al.*^[21,22] reported the formation of an adherent blue-black Fe₃O₄ (magnetite) film, a light brown or a semi-adherent dichroic iron oxide layer on carbon steel in alkaline solutions. They found that a combination of anodization and final sealing with an inhibiting oil had improved the corrosion behavior. The color of surface oxide coatings depends on the film thickness and the viewing angle. Choi *et al.*^[23] developed an anodizing process for pure iron in 25 pct w/v sodium hydroxide solution at 298 K (25 °C) followed by a subsequent annealing. Through their study, it was found that using the highest current density (100 A/dm²) and annealing at 773 K (500 °C) had the best condition for corrosion prevention. Machmudah *et al.*^[24] developed a hydrothermal electrolysis method (anodizing in a batch autoclave) for preparing a magnetite film on mild steel. These experiments conducted in different conditions of current densities, reaction times, electrolyte concentrations, and temperatures. Electrochemical tests showed that these magnetite layers formed on the steel surface could improve its corrosion behavior effectively.

The prior literature investigated the electrochemical behavior of anodized steels in common current densities. Therefore, the main purpose of this study was to evaluate the effect of carbon steel anodic oxidation at high current densities on corrosion behavior. For this purpose, the electrochemical behavior of anodized carbon steel in 3.5 wt pct NaCl solution was investigated by potentiodynamic polarization measurements and EIS.

II. EXPERIMENTAL PROCEDURE

A. Coating Procedure

Carbon steel specimens of 0.5 mm thickness (produced by Mobarakeh Steel Company, Iran) were used throughout the experiments. The detailed composition

ARASH FATTAH-ALHOSSEINI and HAMID YAZDANI KHAN are with the Department of Materials Engineering, Bu-Ali Sina University, Hamedan 65178-38695, Iran. Contact e-mail: hamid.yazdanikhan@gmail.com

Manuscript submitted May 12, 2016.

Article published online February 27, 2017.

Table I. The Composition of Carbon Steel Tested

Element	C	Al	Ni	Cu	Cr	S	P	Si	Mn	Mo	Fe
Composition (Wt Pct)	0.1	0.07	0.02	0.01	0.01	0.01	0.01	0.01	0.55	0.005	bal.

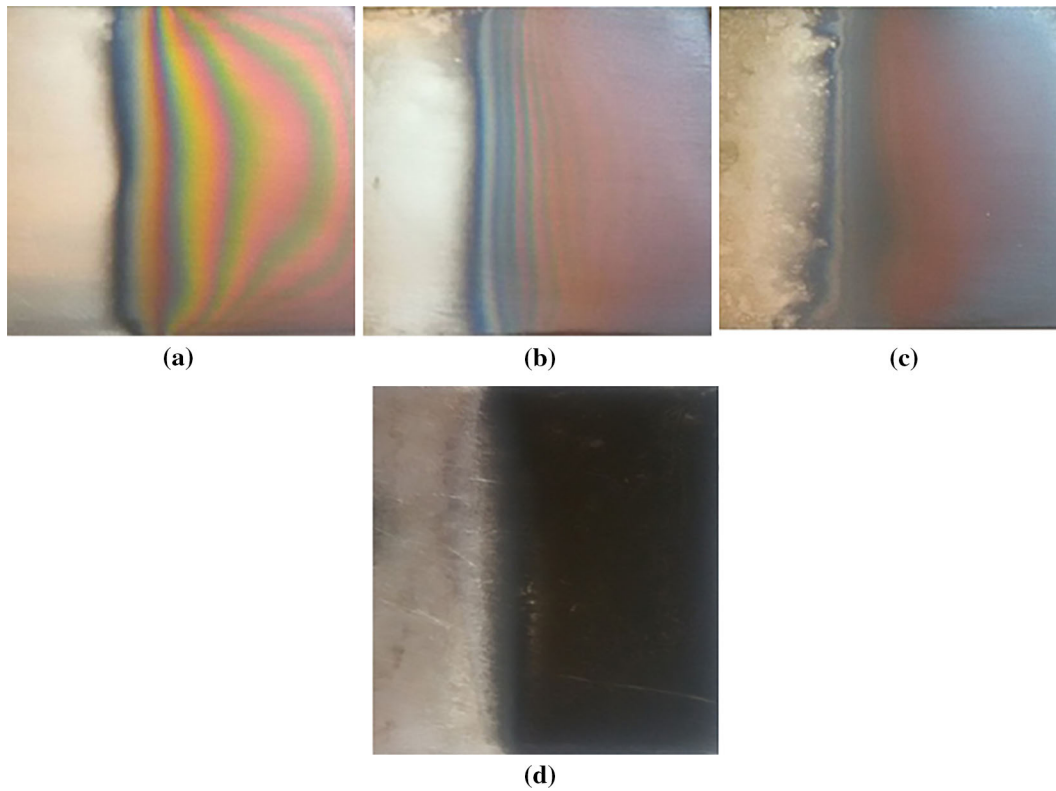


Fig. 1—Photographs of oxide films prepared at (a) 100, (b) 125, (c) 150 A/dm² and (d) cathode.

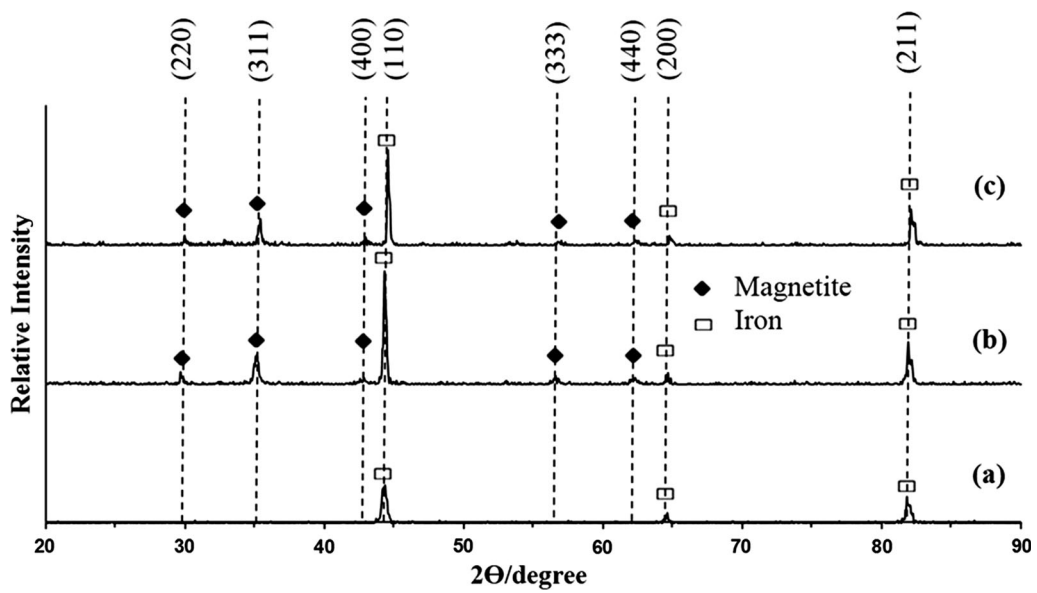


Fig. 2—XRD patterns of (a) base metal, (b) oxide film prepared at 100, and (c) 150 A/dm².

of carbon steel used in this study is given in Table I. All chemicals used in this study were of analytical grade (Merck, Germany). Deionized water was also used throughout the whole experiments. The carbon steel substrates were cut into 20 mm × 35 mm strips and were polished with sand paper (No. 600), rinsed in acetone and ethanol for 15 minutes, and washed with deionized water. Two carbon steel strips were immersed (2 cm²) in a beaker containing 25 pct w/v NaOH solution. The distance between electrodes was fixed at 4 cm. The current densities were adjusted using a Power supply, which was a two-electrode system. Anodization was carried out galvanostatically at constant current densities of 100, 125, and 150 A/dm² at 301 K ± 1 K (28 °C ± 1 °C) for 3600 seconds. During the anodization process, the solution was stirred with a magnetic stir bar. When finished, the coating was washed with deionized water and then dried under a stream of compressed air. All anodized samples were subjected to

a final heat treatment. During the heat treatment for inhibiting of oxidation, the anodized sample was placed into a small cylindrical steel bomb and sealed. The cylindrical bomb was maintained at 773 K (500 °C) for 3600 seconds and then it was allowed to cool down cooled slowly in the air. Finally, the specimens were taken out of the bomb, characterized by XRD, SEM, and electrochemical tests.

B. Coatings Characterization

The surface morphology and cross section of anodic oxide films were characterized using a JEOL JSM-840A scanning electron microscope. Measurement of oxide coating thickness was carried out in accordance with ASTM B 487-85.^[25] The anodized specimens were mounted on edge in cold mounting resin and their surfaces were polished with different grid SiC papers of decreasing grit size (400, 600, 800, 1200, and 2000), then

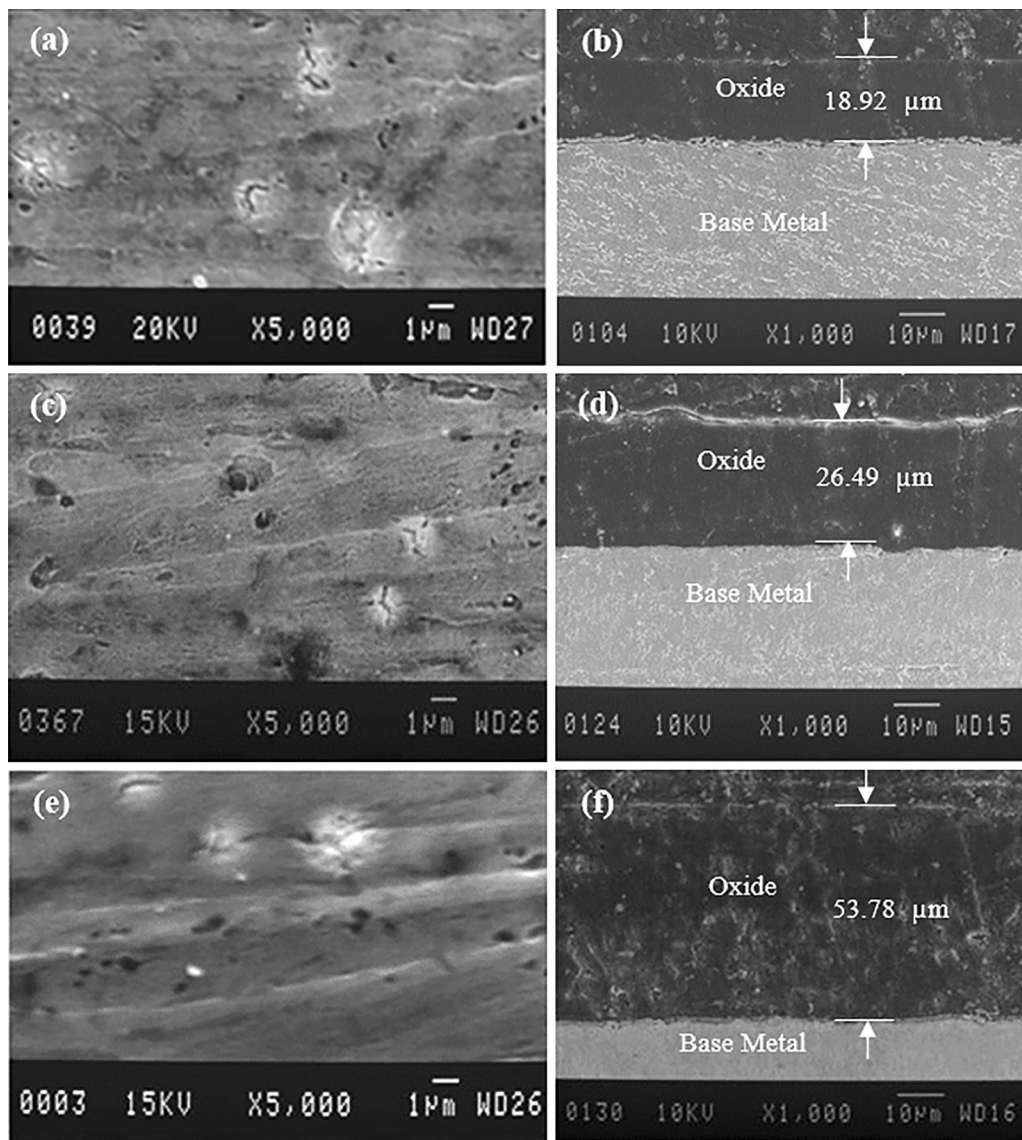


Fig. 3—SEM images of surface and cross section of anodizing films prepared at (a, b) 100, (c, d) 125, and (e, f) 150 A/dm².

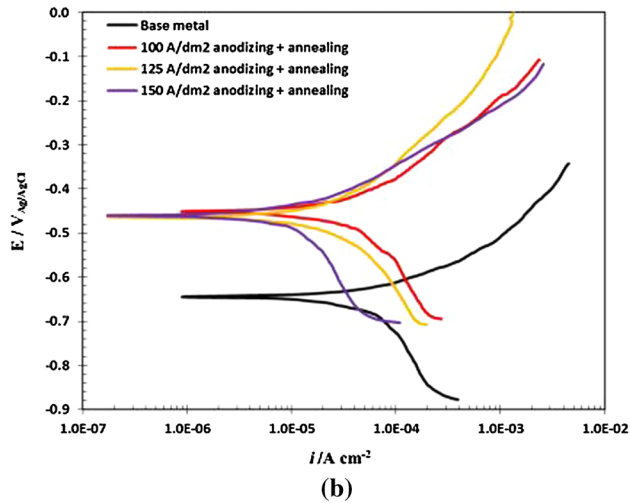
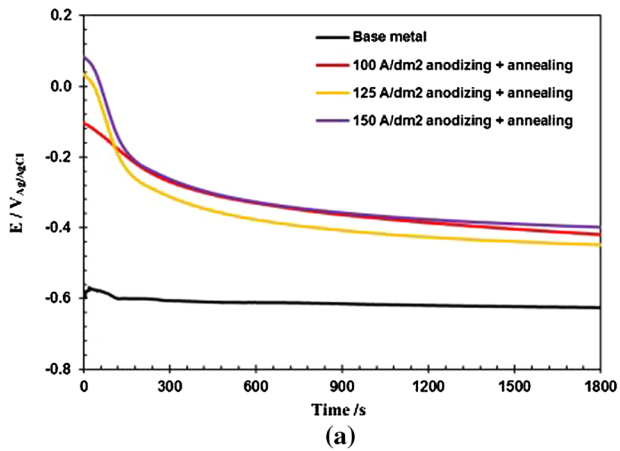


Fig. 4—(a) OCP and (b) potentiodynamic polarization curves of the base metal and anodized carbon steel at 100, 125, and 150 A/dm² in 3.5 wt pct NaCl solution.

etched for 7 seconds in 2 pct Nital. For increasing the conductivity during microscopy imaging, the cold mounting resin specimens were covered with thin gold films by JEOL JFC-1100E ion sputtering system. Phase identification of coatings was carried out with XRD method by an Italstructures APD2000 diffractometer using CuK_α radiation ($\lambda = 1.54178 \text{ \AA}$) with diffraction angle 2θ : 20 to 90 deg and the data were analyzed by a X'Pert HighScore Plus software.

C. Electrochemical Measurements

The electrochemical tests of the bare steel sample and the anodic coatings were performed using a μ Autolab Type III/FRA2 system controlled by a personal computer. The working, counter, and reference electrodes were the anodized carbon steel, Pt plate, and Ag/AgCl saturated in KCl, respectively. For all specimens, testing O-ring surface area of approximately 0.4 cm² was exposed to the 3.5 wt pct NaCl solution (artificial sea water solution) for 1800 seconds before corrosion tests. The EIS test was carried out in the frequency range of 100 kHz to 10 mHz at open circuit potential (OCP) with an amplitude of 10 mV. Also, potentiodynamic

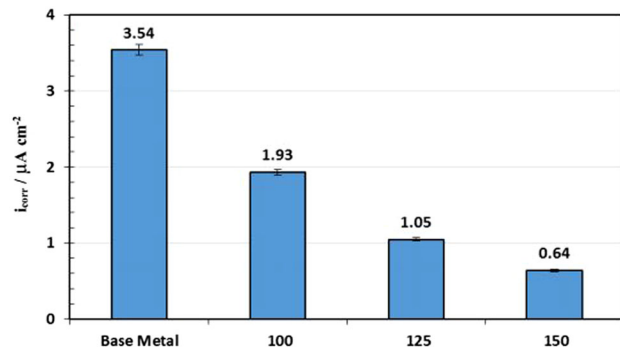
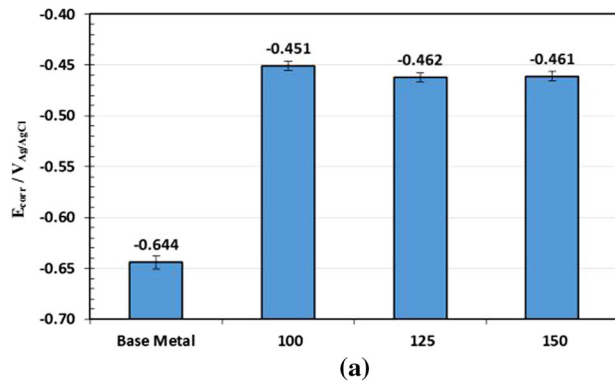


Fig. 5—Variations of the (a) corrosion potential and (b) corrosion current density of the base metal and anodized carbon steel at 100, 125, and 150 A/dm² in 3.5 wt pct NaCl solution.

polarization measurements were performed at a scan rate of 1 mV/s.^[26–28] The corrosion current density (i_{corr}) was measured by Tafel extrapolation of the linear part of the cathodic branch back to the corrosion potential.^[26–28] Each electrochemical measurement was repeated at least three times.

III. RESULTS AND DISCUSSION

A. Appearance of Oxide Films

As shown in Figures 1(a) through (c), oxide films were prepared on the carbon steel surface in 25 pct w/v sodium hydroxide solution by anodizing process. When the current density was increased and other parameters were kept fixed, the carbon steel surface color became dark. Interestingly, the obtained results are similar to the previous works which were reported by Burleigh *et al.*^[21,22] and Machmudah *et al.*^[24] Indeed, diverse range of colors appeared on the carbon steel surface depending on the thickness of anodic oxide film.^[29–31] As time progressed, a black deposit formed on the surface of the cathode (Figure 1(d)). The cathode was black in appearance as a consequence of iron ions reduction on carbon steel surface. The cathodic film grew large enough beyond what could be removed by simply touching the surface. In general, different colors are formed owing to:

1. In low film thicknesses: Interference of light reflected at the oxide film/air and steel/oxide film

interfaces, resulting from different thicknesses of the oxide film on carbon steel surface.^[29–31]

2. In high film thicknesses: The interference of light is not possible. Thus, in our work by increasing the thicknesses of oxides (increasing the current density), the anodized samples become dark and turn to the original color of magnetite (black).

B. XRD Characterizations

Figures 2(a) through (c), respectively, describes the XRD patterns of the carbon steel substrate, anodic oxide film prepared at current densities of 100 and 150 A/dm². According to Figure 2(a), all peaks can be indexed to iron. Both 100 and 150 A/dm² anodized samples show the same relative intensities of magnetite (Fe₃O₄) and iron peaks. Thus, the ratio of magnetite and iron in coatings was not changed by applying different current densities, but the thickness of oxide film was increased. (This will be discussed later in Section III–C.) In fact, by increasing the current density in anodizing process, the amount of iron and magnetite was increased but the ratio remained the same. Also, Choi *et al.*^[23] found similar results in anodization of pure iron. Moreover, the XRD patterns did not reveal the presence of hematite peaks which are quite deleterious to the corrosion resistance.^[32]

C. SEM Observations

The first and the second columns in Figure 3 depict characteristic top views of SEM images and corresponding cross-section views of different anodized films. Figures 3(a), (c), and (e) show the surface morphologies of the anodized surfaces of carbon steel at different current densities. It can be seen that the surface morphologies of all coatings show similar features which are associated with a few number of fine cracks. The heat treatment may have induced these fine cracks. Nevertheless, bearing in mind that the anodic oxide film is an amorphous phase which naturally contains numerous structural defects, heat treatment seems to be an essential step to eliminate these defects and induce crystallinity to some extent, thereby, enhancing its overall corrosion resistance.^[21–23] The fact that whether or not these cracks pose serious detrimental effects on the overall corrosion resistance will be further elucidated in the course of our subsequent electrochemical analyses. Furthermore, the cross-section views of these coatings (Figures 3(b), (d), and (f)) show the anodizing films that are continuous and fairly uniform in thickness. Evidently, the thickness of oxide film has increased by anodizing at constant current densities of 100, 125, and 150 A/dm² in alkaline solution. As explained by Choi *et al.*^[23] and Machmudah *et al.*,^[24] the thickness of protective oxide film was proportional to the applied current density. Therefore, as the current density increased, the built-in potential increased (anodic forming voltage). In other words, the anodic forming voltage has increased for coatings as a function of current density.

D. Electrochemical Tests

Figure 4(a) shows the OCP plots of the base metal and anodized carbon steel at 100, 125, and 150 A/dm² in 3.5 wt pct NaCl solution. As is evident in Figure 4(a), all

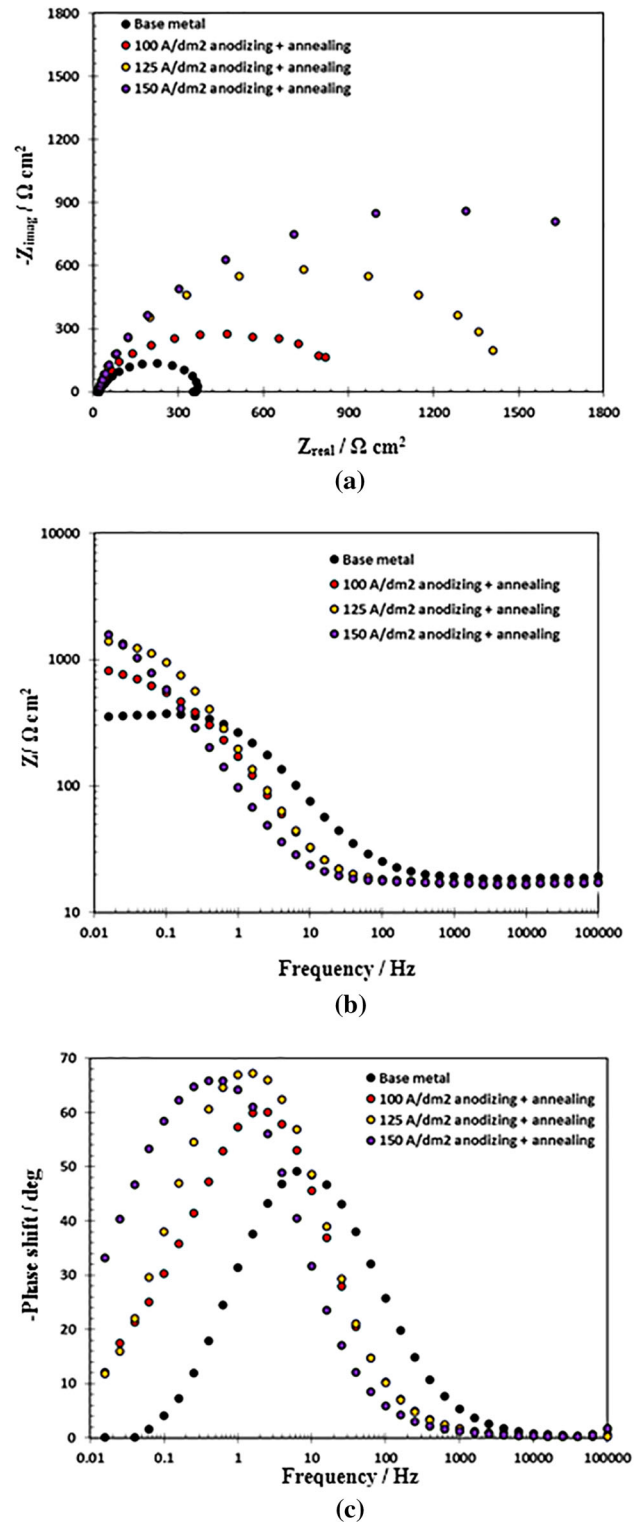


Fig. 6—(a) Nyquist, (b) Bode, and (c) Bode-phase plots of carbon steel with and without anodic oxide coatings in 3.5 wt pct NaCl solution.

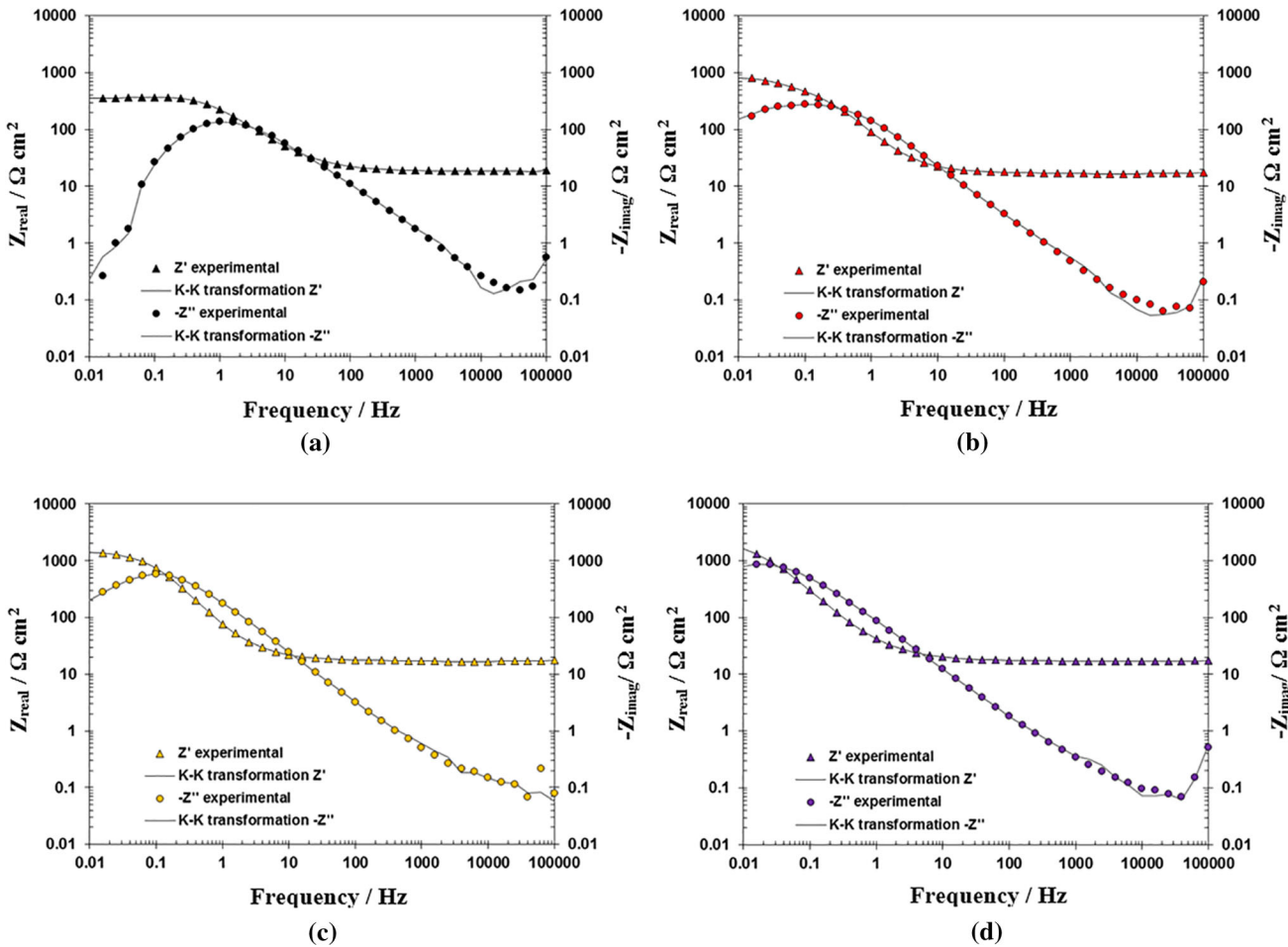


Fig. 7—Kramers–Kronig (K–K) transformation of the EIS data obtained for (a) base metal, anodized carbon steel at (b) 100, (c) 125, and (d) 150 A/dm² in 3.5 wt pct NaCl solution.

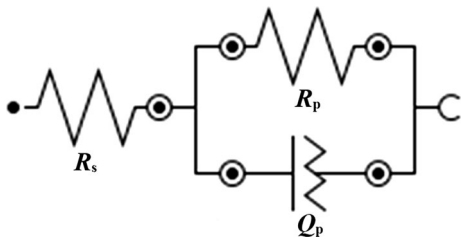


Fig. 8—The best equivalent circuit used to model the experimental EIS data.

plots reveal similar trends of reduction in the potential toward the negative values. Moreover, Figure 4(a) depicts that stable condition was obtained after 1800 seconds in order to implement the electrochemical tests. In fact, after 1500 seconds, the variation of potential with time is very slight verifying that steady state conditions dominated. Reaching a stable OCP in a short period of time has also been found by other researchers.^[16,32]

The potentiodynamic polarization curves of the base metal sample and those which were anodized at three different current densities of 100, 125, and 150 A/dm² are all shown in Figure 4(b). All samples exhibit the

same curve shapes where the current changes smoothly and linearly around the corrosion potential demonstrating cathodic and anodic Tafel behaviors. For the sake of clarity, corrosion potentials and corrosion current densities derived from above curves are shown as two histograms in Figure 5. The obtained results revealed that anodization at aforementioned current densities had two important aspects. First, the anodized samples showed higher nobler values of corrosion potential (Figure 5(a)). Second, anodization lowered the corresponding corrosion current densities. Obviously, anodization at the highest current density resulted in a sample which has the lowest corrosion current density. Thus, it was expected that this sample would have the highest corrosion resistance. Nonetheless, this inference needs further electrochemical tests to support it.

EIS analysis was performed for the base metal sample and all anodized samples at OCP condition in 3.5 wt pct NaCl solutions, and the obtained results are all shown as Nyquist, Bode-magnitude, and Bode-phase plots in Figure 6. Considering Figure 6(a), all Nyquist plots show imperfect depressed semicircles. Since the diameters of these semicircles are directly proportional to their corresponding overall resistance, galvanostatic anodization at 150 A/dm² yields a sample which has the highest

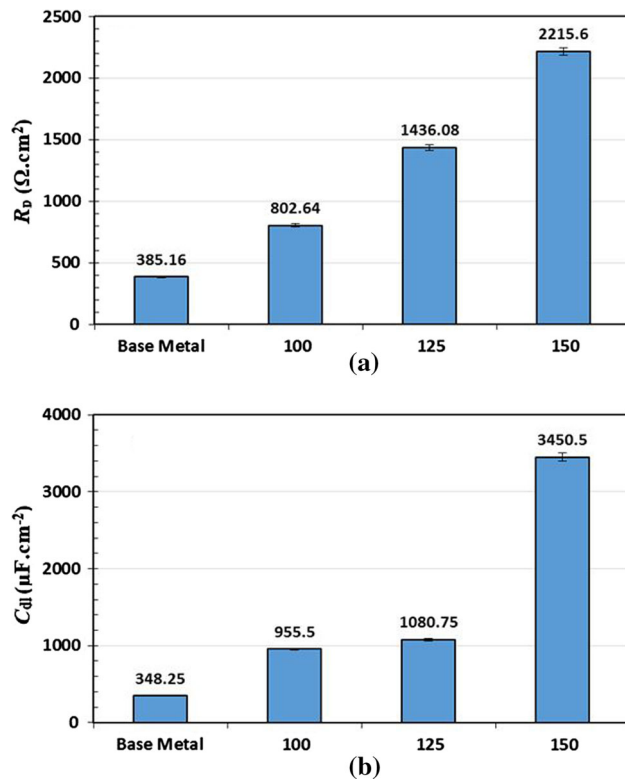


Fig. 9—Impedance parameters derived from EIS results: (a) polarization resistance and (b) double-layer capacitance.

resistance. On the other hand, both Bode plots demonstrate a resistive behavior at high frequencies, whereas a marked capacitive behavior is evident in the middle to low frequency range for all samples (Figures 6(b) and (c)). Besides, Bode-phase plots show a single time constant (only one maximum phase lag at the middle-frequency range). In this manner, the phase angle values remained close to -90 deg and revealed the formation and growth of an oxide passive film.^[33] Also, as is evident in Figure 6(c), the phase angle maxima is lower than -90 deg; such behaviors can be explained as a deviation from an ideal capacitor behavior.^[34,35]

Before going any further, it is worth checking the reliability of impedance data. For this purpose, the electrochemical system needs to fulfill the linear system theory constraints, which are namely causality, linearity, and stability. To test and validate the experimental impedance data, Kramers–Kronig (K-K) transforms were applied. In this method, the real axis is transformed to imaginary axis and vice versa. A full description of K-K transforms as well as accompanied formulations can be found elsewhere.^[34–37] The EIS experimental data of the base metal sample and those which were anodized galvanostatically were compared with those resulted from K-K transforms (Figure 7). The obtained results show the agreement between the experimental data and K-K transforms, which accorded well with the linear system theory.

An equivalent electrical circuit (EEC), shown in Figure 8 (with one time constant), was used here to describe the impedance spectra.^[34,38] In this EEC, Q_p is the constant phase element (CPE), R_p is the polarization

resistance, and R_s represents the solution resistance ($R_s = 17.5 \pm 0.4 \Omega \cdot \text{cm}^2$). For a circuit including a CPE, the capacitance (C) can be calculated from Eq. [1]^[39]:

$$C = Y_0(\omega_c)^{n-1}, \quad [1]$$

where Y_0 is the CPE constant in terms of admittance, ω_c is the critical angular frequency (rad s^{-1}) at which the imaginary part of the impedance has a maximum, n is a parameter related to surface roughness. It is worth noting that the above critical angular frequency (ω_c) can be calculated from Eq. [2]^[39]:

$$\omega_c = \left(\frac{1}{R_p Y_0} \right)^{1/n}, \quad [2]$$

where R_p is the polarization resistance and other parameters have the same meanings as before. The variation of impedance parameters for base metal and anodized samples in 3.5 wt pct NaCl solution are depicted as histograms in Figure 9. Among all, the one that was anodized at the highest current density, 150 A/dm², has the highest polarization resistance and double-layer capacitance. Accordingly, all electrochemical tests indicated that the highest applied current density used in this work yields an anodic oxide film which is superior passivity and the best corrosion resistance. In this respect, Choi *et al.* came to an analogous conclusion but for different current densities of anodization and heat treatment procedure.^[23] In contrast to their work, however, the anodic coatings obtained herein were thicker by several orders of magnitude.

Interestingly, the aforementioned fine cracks had no adverse effect on the overall corrosion resistance. From another angle, however, no one would expect the occurrence of galvanic corrosion if these fine cracks were deep enough to reach the substrate. This seems reasonable when one considers the electrochemical similarity between the anodic oxide film and natural passive film of carbon steel. On the whole, galvanostatic anodization of carbon steel followed by a final heat treatment, such as discussed above, seems to be efficient, fast, cost-effective, and environmentally benign in order to enhance the corrosion resistance of carbon steel.

IV. CONCLUSIONS

The most important results obtained by studying the anodization process of carbon steel at high current densities can be summarized as follows:

1. Thick protective oxide films were successfully obtained by anodization at high current densities on the surface of carbon steel. As the current density increased, the built-in potential and the oxide growth increased. Different oxide film thicknesses led to the appearance of different colors on the surface of the sample.
2. The anodic films produced on carbon steel were composed essentially of iron and magnetite. The absence of undesirable hematite phase was confirmed by XRD patterns.

3. Potentiodynamic polarization curves indicated that implementing the anodizing process followed by heat treatment markedly decreased the corrosion rate of this coating.
4. EIS results showed that as the current density increased, the charge-transfer resistance increased.

REFERENCES

1. M. Schwartz: *Encyclopedia of Materials, Parts, and Finishes*, CRC Press, USA, 2002, pp. 55–59.
2. X. Zhou, P.G. Sheasby, and B.A. Scott: *Coatings Produced by Anodic Oxidation, Surface Treatment and Modification*, University of Manchester, Manchester, 2010, pp. 2503–18.
3. J. Weber, and T. Biestek: *Electrolytic and Chemical Conversion Coatings: A Concise Survey of Their Production, Properties and Testing*, Portcullis Press, Redhill, 1976, pp. 112–13.
4. S.-I. Yamazaki, N. Fujiwara, and K. Yasuda: *Electrochim. Acta*, 2010, vol. 55, pp. 753–58.
5. Z. Zhang, M.F. Hossain, and T. Takahashi: *Applied Catalysis B: Environmental*, 2010, vol. 95, pp. 423–29.
6. C.Y. Chang, C.H. Wang, C.J. Tseng, K.W. Cheng, L.W. Hourng, and B.T. Tsai: *Int. J. Hydrog. Energy*, 2012, vol. 37, pp. 13616–22.
7. Y. Konno, E. Tsuji, P. Skeldon, G.E. Thompson, and H. Habazaki: *J. Solid State. Electrochem.*, 2012, vol. 16, pp. 3887–96.
8. K. Xie, M. Guo, H. Huang, and Y. Liu: *Corros. Sci.*, 2014, vol. 88, pp. 66–75.
9. M.M. Momeni, Y. Ghayeb, and F. Mohammadi: *J. Mater. Sci.: Mater. Electron.*, 2015, vol. 26, pp. 685–92.
10. Y. Konno, S. Yang, E. Tsuji, Y. Aoki, P. Skeldon, G.E. Thompson, and H. Habazaki: *J. Electrochem. Soc.*, 2013, vol. 50, pp. 183–90.
11. H. Deng, M.C. Huang, W.H. Weng, and J.C. Lin: *Surf. Coat. Technol.*, 2015, vol. 266, pp. 183–87.
12. K. Xie, J. Li, Y. Lai, W. Lu, Z. Zhang, Y. Lui, L. Zhou, and H. Huang: *Electrochem. Commun.*, 2011, vol. 13, pp. 657–60.
13. F. Boudoire, R. Toth, J. Heier, A. Braun, and E.C. Constable: *Appl. Surf. Sci.*, 2014, vol. 305, pp. 62–66.
14. J. Chen, K. Huang, and S. Liu: *Electrochim. Acta*, 2009, vol. 55, pp. 1–5.
15. H. Zhu, D. Yang, and L. Zhu: *Surf. Coat. Technol.*, 2007, vol. 201, pp. 5870–74.
16. H. Zhu, F. Cao, D. Zuo, L. Zhu, D. Jin, and K. Yao: *Appl. Surf. Sci.*, 2008, vol. 254, pp. 5905–09.
17. D.B. Vershok, P.I. Misurkin, V.A. Timofeeva, A.B. Solov'eva Yu. I. Kuznetsov, and S.F. Timashev: *Protect. Met.*, 2008, vol. 44, pp. 721–28.
18. Y.I. Kuznetsov, D.B. Vershok, S.F. Timashev, A.B. Solov'eva, P.I. Misurkin, V.A. Timofeeva, and S.G. Lakeev: *Russian J. Electrochem.*, 2010, vol. 46, pp. 1155–66.
19. H. Tamura: *Corros. Sci.*, 2008, vol. 50, pp. 1872–83.
20. R.W. Revie and H.H. Uhlig: *Corrosion and Corrosion Control*, Wiley, Hoboken, NJ, 2008, pp. 115–16.
21. T.D. Burleigh, T.C. Dotsen, K.T. Dotsen, S.J. Gabay, T.B. Sloan, and S.G. Ferrell: *J. Electrochem. Soc.*, 2007, vol. 154, pp. C579–C586.
22. T.D. Burleigh, P. Schmuki, and S. Virtanen: *J. Electrochem. Soc.*, 2009, vol. 156, pp. C45–C53.
23. Y.W. Choi, S. Shin, D.W. Park, and J. Choi: *Curr. Appl. Physics*, 2014, vol. 14, pp. 641–48.
24. S. Machmudah, R. Zulhijah, H. Wahyudiono, H.Kanda. Setyawan, and M. Goto: *Chem. Eng. J.*, 2015, vol. 268, pp. 76–85.
25. ASTM B 487-85: *Standard Test Method for Measurement of Metal and Oxide Coating Thickness by Microscopical Examination of a Cross Section*, ASTM International, Philadelphia, 2007, pp. 1–4.
26. S.O. Gashti and A. Fattah-Alhosseini: *Anal. Bioanal. Electrochem.*, 2014, vol. 6, pp. 535–546.
27. A. Fattah-alhosseini and S.O. Gashti: *J. Mater. Eng. Perform.*, 2015, vol. 24, pp. 3386–93.
28. O. Imantalab and A. Fattah-alhosseini: *J. Mat. Eng. Perform.*, 2015, vol. 24, pp. 2579–85.
29. K.O. Vasconcelos, N. Bocchi, R.C. Rocha-Filho, and S.R. Biaggio: *J. Electrochem. Soc.*, 2005, vol. 152, pp. B491–B494.
30. H. Xin-kuai, C. Bai-zhen, L. Xiao-dong, H. Geng-sheng, W. Lu-ye, and T. Wen-Zeng: *J. Central South Univer. Technol.*, 2006, vol. 13, pp. 135–40.
31. J. Corredor, C.P. Bergmann, M. Pereira, and L.F.P. Dick: *Surf. Coat. Technol.*, 2014, vol. 245, pp. 125–32.
32. A. Fattah-alhosseini, H. Yazdani Khan, and A. Heidarpour: *J. Alloys Compd.*, 2016, vol. 676, pp. 474–80.
33. A. Fattah-alhosseini and O. Imantalab: *Metall. Mater. Trans. A*, 2016, vol. 47A, pp. 572–80.
34. F.R. Attarzadeh, N. Attarzadeh, S. Vafaeian, and A. Fattah-Alhosseini: *J. Mat. Eng. Perform.*, 2016, vol. 25, pp. 4199–209.
35. A. Fattah-alhosseini, O. Imantalab, and F.R. Attarzadeh: *Metall. Mater. Trans. B*, 2016, vol. 47B, pp. 2761–70.
36. M. Schönleber, D. Klotz, and E. Ivers-Tiffée: *Electrochim. Acta*, 2014, vol. 131, pp. 20–27.
37. A. Fattah-alhosseini and S. Vafaeian: *Appl. Surf. Sci.*, 2016, vol. 360, pp. 921–28.
38. E. Onofre-Bustamente, M.A. Domínguez-Crespo, J. Genescá-Llongueras, and F.J. Rodríguez-Gómez: *Surf. Coat. Technol.*, 2007, vol. 201, pp. 4666–76.
39. S.P. Harrington and T.M. Devine: *J. Electrochem. Soc.*, 2008, vol. 155, pp. C381–C386.